Electronic Supplementary Information (ESI)

Sulfite Modification of Platinum Nanoparticles Modulates Electrocatalytic Formic Acid Oxidation Activity

Moxuan Liu, Shumeng Zhang, Zhixue Zhang, Zhaojun Liu, Kai Liu, and Chuanbo Gao*

Center for Materials Chemistry, Frontier Institute of Science and Technology, and State Key Laboratory of Multiphase Flow in Power Engineering, Xi'an Jiaotong University, Xi'an, Shaanxi 710054, China.

Email: gaochuanbo@mail.xjtu.edu.cn

Additional Experimental Details

Materials. Commercial Pt/C (20 wt%, from Johnson Matthey), sodium sulfite (Na_2SO_3), sulfuric acid (H_2SO_4), formic acid (HCOOH), sodium borohydride ($NaBH_4$), polyvinylpyrrolidone (PVP) (Mw 40,000), and chloroplatinic acid (H_2PtCl_6) were purchased from Sigma-Aldrich. All chemicals were used as purchased without further purification.

Preparation of Pt NPs-SO_3^{2-}. Pt nanoparticles were first synthesized by injecting 0.5 mL of $NaBH_4$ (0.1 M) into 4.5 mL of a mixed solution containing 0.022 wt% PVP (Mw 40,000) and 4.4 mM H_2PtCl_6. The reaction solution was stirred vigorously at 25 °C for 10 min. The Pt nanoparticles were collected by centrifugation, washed three times with H_2O, and redispersed in 1 mL of H_2O. Then, sulfite was modified on the Pt nanoparticles by immersing them in 0.5 M Na_2SO_3 for 2 h, collected by centrifugation, and washed thoroughly with H_2O. Alternatively, Pt NPs-SO_3^{2-} can be synthesized by following the same procedures as the synthesis of Pt/C-SO_3^{2-}, which involves electrocatalytic activation of the Pt nanoparticles before the adsorption of SO_3^{2-}.

Electrode Preparation and Electrocatalytic Measurements. The experimental details are described in the Experimental Section. Scheme 1 summarizes the typical processes involved in the experiments.

Scheme S1. Experimental procedures of the electrocatalysis

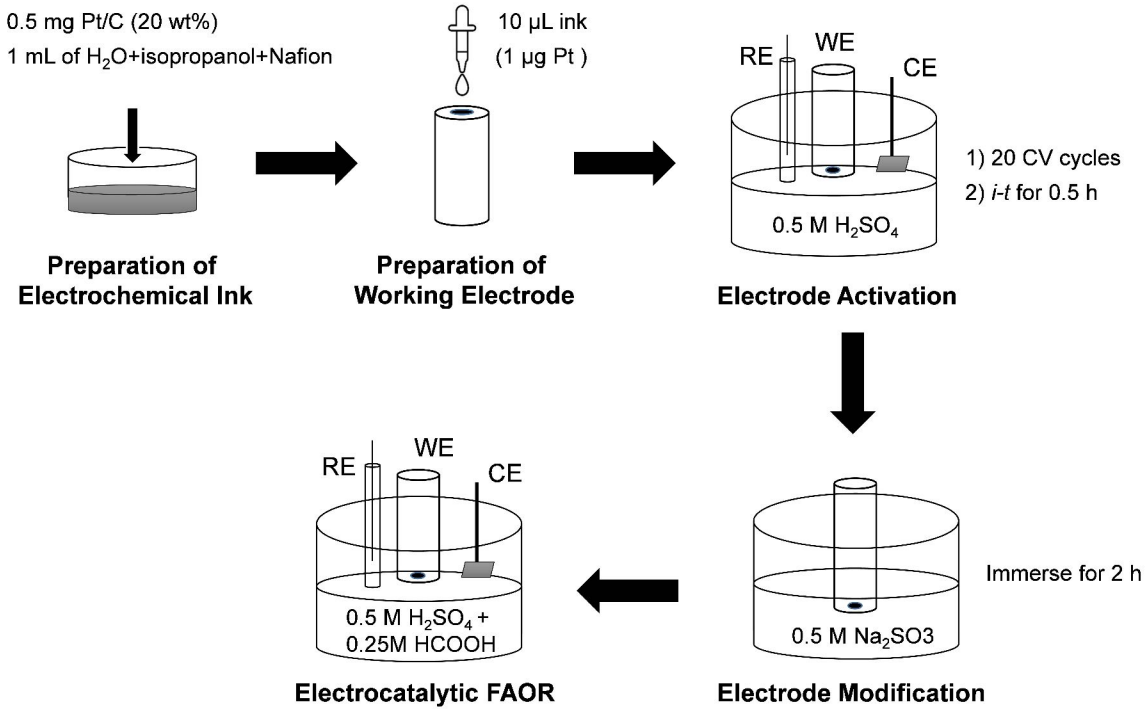

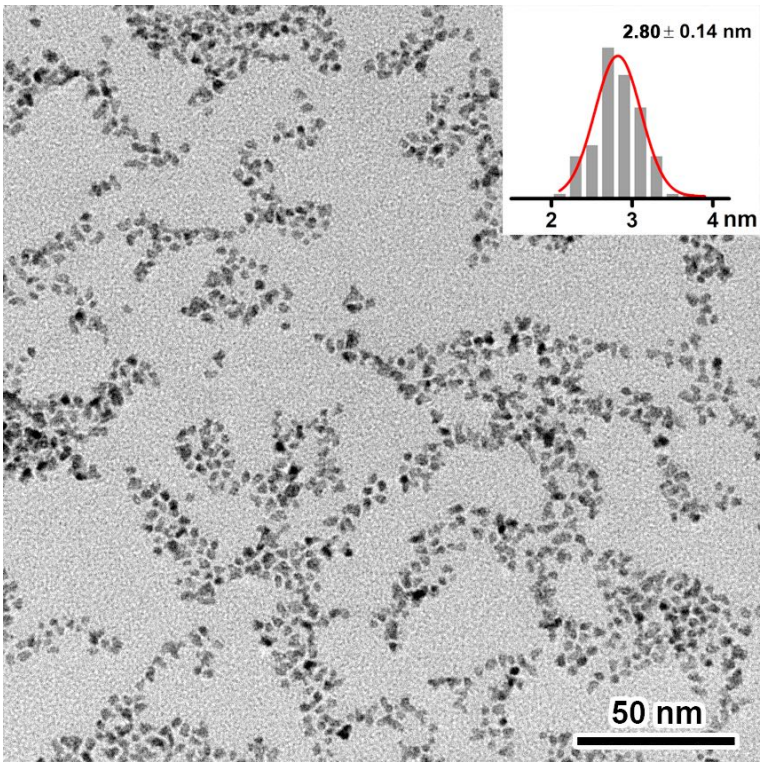

Fig. S1 TEM image of Pt nanoparticles (Pt NPs) before the sulfite modification. Inset: size distribution of the Pt NPs.

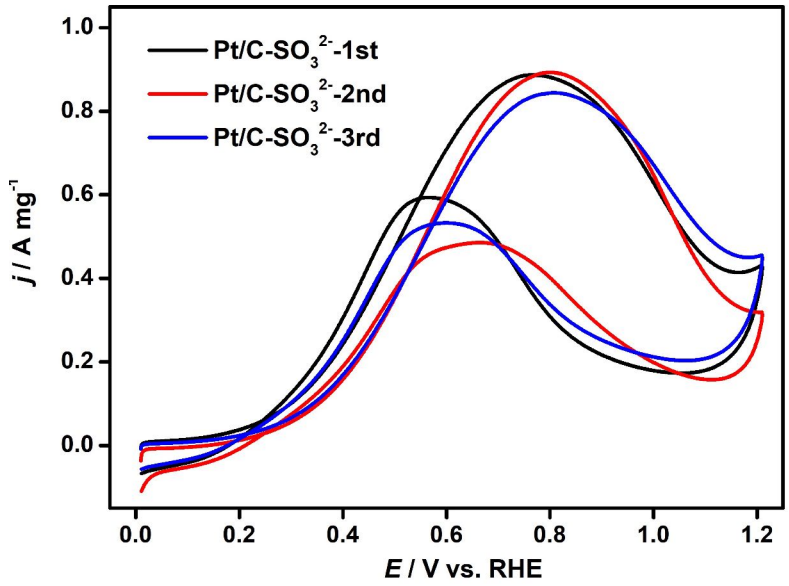

Fig. S2 Reproducibility of the FAOR activities of the Pt/C-SO_3^{2-} catalyst. CV curves were obtained with three parallel samples in N_2-saturated 0.25 M HCOOH + 0.5 M H_2SO_4 at a scan rate of 50 mV s^{-1}. It indicates that the electrocatalytic activities are highly reproducible. The mass activities of the Pt/C-SO_3^{2-} catalyst at 0.55 V vs. RHE were 0.597, 0.478, and 0.472 A mg^{-1}, respectively, showing a standard deviation of 0.070 A mg^{-1}.

Table S1. Reproducibility of the electrocatalytic activities, showing the specific and mass activities of the catalysts at 0.55 V vs. RHE measured from three parallel samples.

Catalysts	Specific activities / mA cm^{-2}		Mass activities / A mg^{-1}	
Pt/C	0.0666	0.0642±0.0023	0.0864	0.0833±0.0029
	0.0639		0.0829	
	0.0621		0.0806	
$Pt/C\text{-}SO_3^{2-}$	0.991	0.856±0.117	0.597	0.516±0.070
	0.793		0.478	
	0.783		0.472	

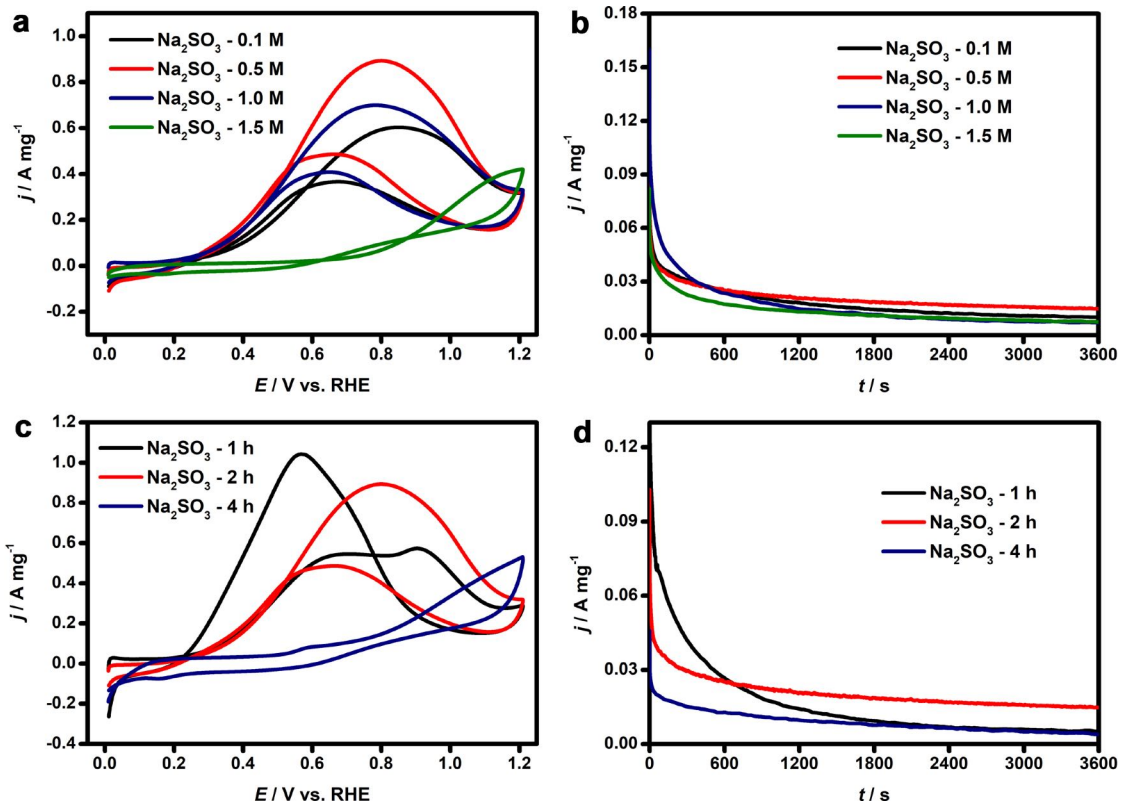

Fig. S3 Performance of the Pt/C-SO_3^{2-} catalyst prepared under different conditions in the electrocatalytic FAOR. (a, c) CV curves of the catalysts in N_2-saturated 0.25 M HCOOH + 0.5 M H_2SO_4 at a scan rate of 50 mV s^{-1}. (b, d) Chronoamperometric *i-t* curves of the catalysts in N_2-saturated 0.25 M HCOOH + 0.5 M H_2SO_4 at 0.345 V vs. RHE. Conditions: (a, b) The concentration of Na_2SO_3 was changed from 0.1 M to1.5 M while the adsorption time was maintained to be 2 h. (c, d) The adsorption time was varied while the concentration of Na_2SO_3 was maintained to be 0.5 M.

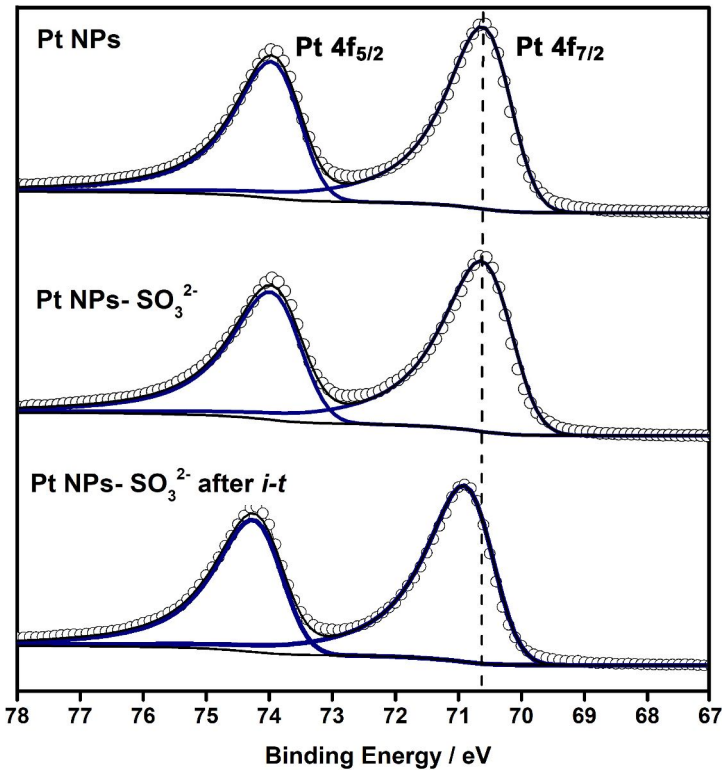

Fig. S4 Core-level Pt 4f XPS spectra of the Pt NPs, the Pt NPs-SO_3^{2-} as prepared, and the Pt NPs-SO_3^{2-} after 1 h of the *i–t* test at 0.345 V vs. RHE. One set of $4f_{5/2}$ and $4f_{7/2}$ can be used to fit the peaks in all the spectra. After modification of the Pt NPs by SO_3^{2-}, the peak positions were almost unchanged, which indicates that the electronic structure of the Pt NPs was not significantly altered during the modification process. After the FAOR (*i–t* test at 0.345 V for 1 h), the XPS peaks shifted to the high binding energies. It can be inferred from the S 2p XPS that S^{2-} forms on the Pt surface during the *i–t* test (Fig. 4b), which is supposed to contribute to the change of the oxidation state of Pt on the surface and thus its XPS spectrum.

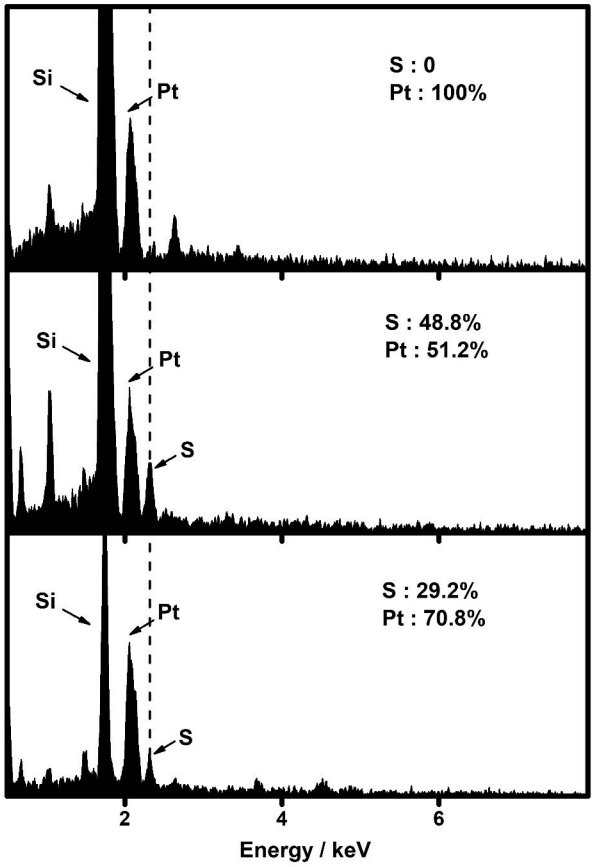

Fig. S5 EDS of the Pt NPs (top), the Pt NPs-SO_3^{2-} as prepared (middle), and the Pt NPs-SO_3^{2-} (bottom) after 1 h of the *i-t* test.

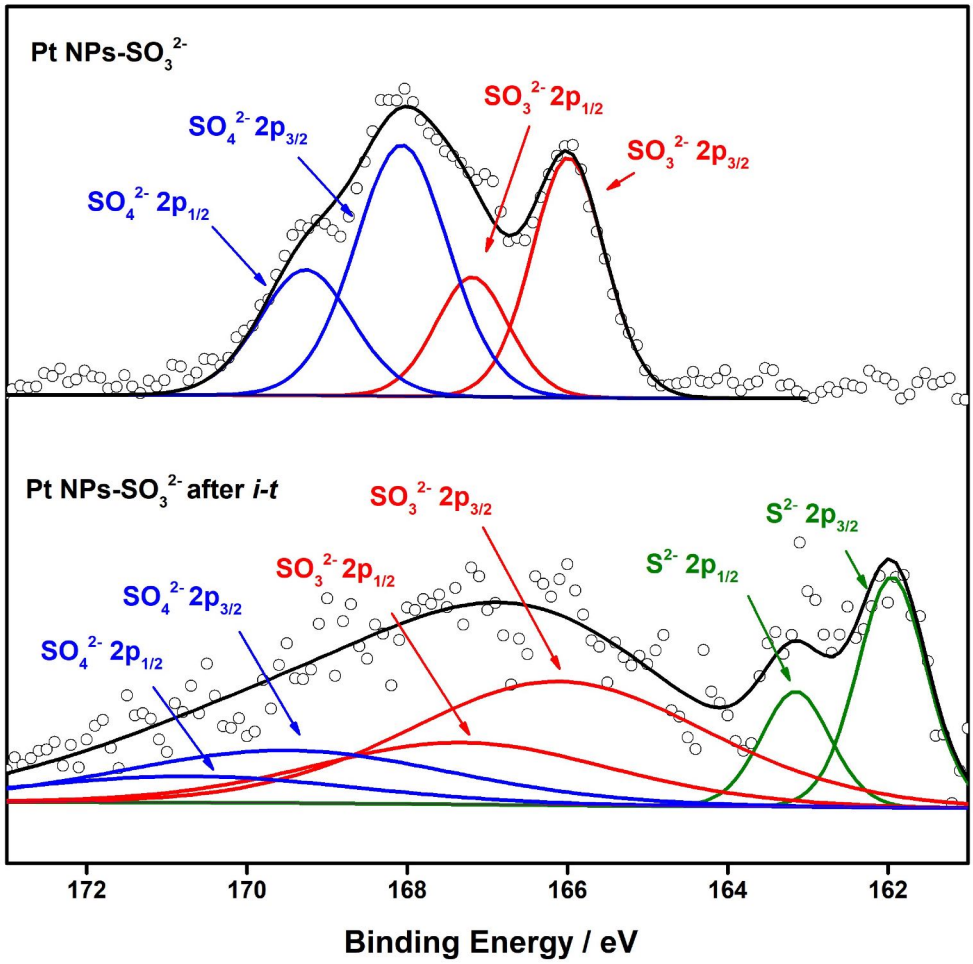

Fig. S6 Comparison of the core-level S 2p XPS of the Pt NPs-SO_3^{2-} as prepared and the Pt NPs-SO_3^{2-} after 1 h of the *i–t* test at 0.345 V vs. RHE.

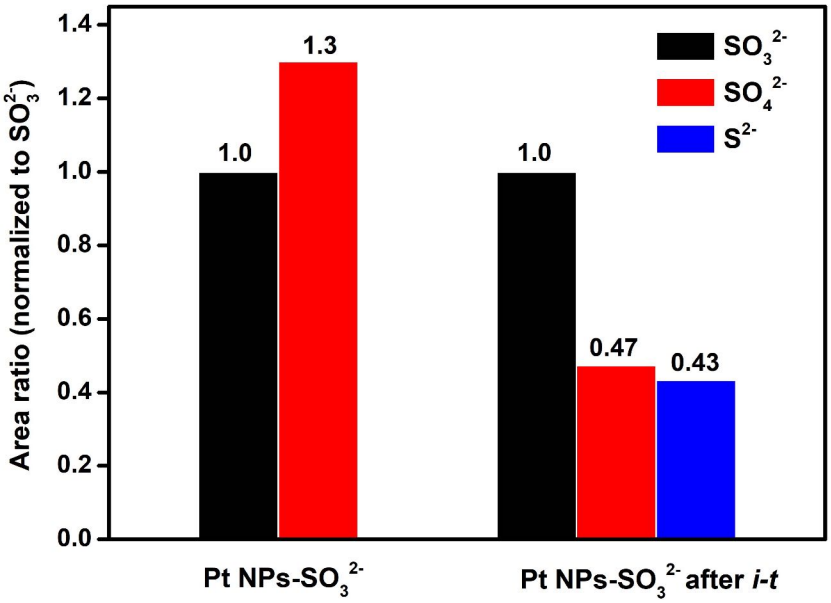

Fig. S7 Change of the S 2p XPS spectra of the Pt NPs-SO_3^{2-} catalyst before and after 1 h of the *i-t* test (original spectra, see Fig. 1g, 4b, or Fig. S6). The peak area of SO_3^{2-} was set to unity (1.0). This figure shows the peak area ratios of SO_4^{2-}/SO_3^{2-} and S^{2-}/SO_3^{2-}. After the *i-t* test, the ratio of SO_4^{2-}/SO_3^{2-} decreased, indicating the detachment of SO_4^{2-} from the Pt surface due to the weak adsorption energy. S^{2-} species emerged with a S^{2-}/SO_3^{2-} ratio of 0.43, which may result from the disproportionation reaction of SO_3^{2-}.

Table S2. Atomic fractions of S and Pt in the Pt NPs-SO_3^{2-} catalyst before and after 1 h of the *i-t* test, derived from the XPS data.

Catalysts	XPS	Atomic fraction (%)
Pt NPs-SO_3^{2-}	S 2p	41.1
	Pt 4f	58.9
Pt NPs-SO_3^{2-} after 3600 s of the *i-t* test	S 2p	24.9
	Pt 4f	75.1

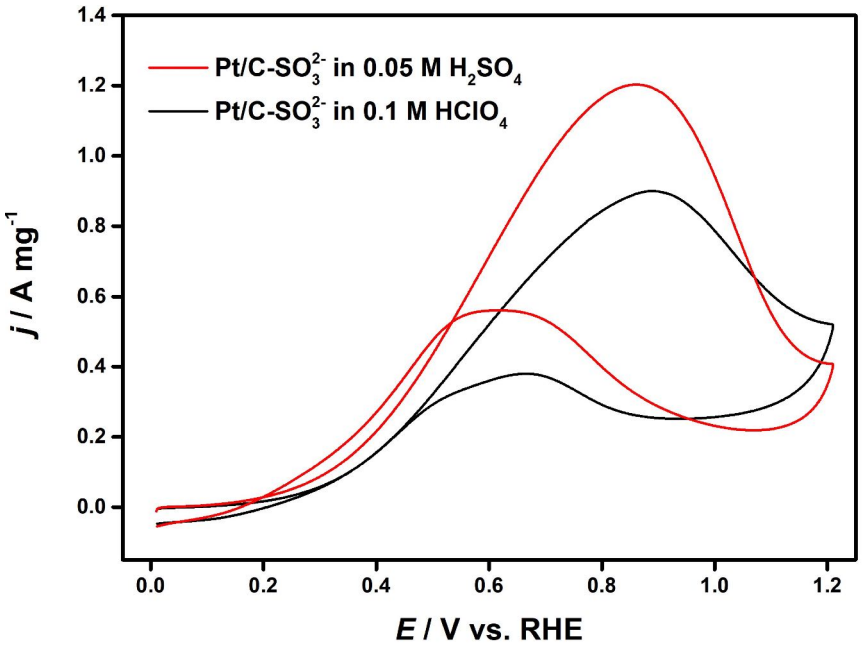

Fig. S8 Effect of SO_4^{2-} on the electrocatalytic activity. Comparison of the FAOR activity of the Pt/C-SO_3^{2-} catalyst in 0.25 M HCOOH + 0.1 M $HClO_4$ and in 0.25 M HCOOH + 0.05 M H_2SO_4. Scan rate: 50 mV s^{-1}. The acidity of the electrolytes was kept constant, while the latter contains a high concentration of SO_4^{2-} that can be adsorbed on the surface of the Pt catalyst. It is reasonable that the SO_4^{2-} helps to decrease the size of the Pt ensembles, albeit the weak adsorption energy, which further contributed to the suppression of the dehydration of formic acid and therefore enhanced FAOR activity.

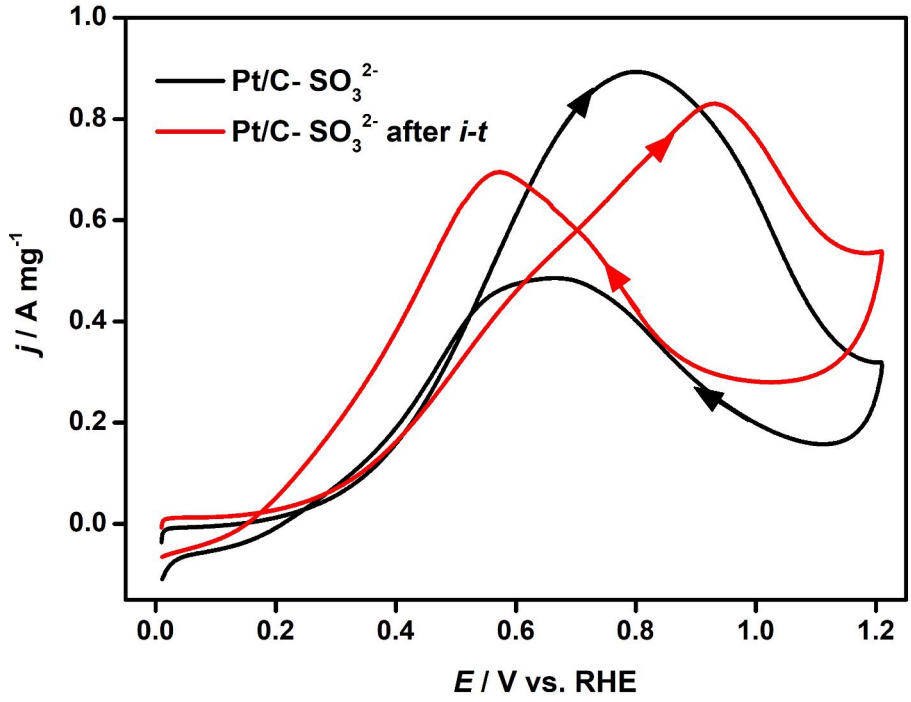

Fig. S9 Comparison of the FAOR activity of the Pt/C-SO_3^{2-} catalyst before and after 1 h of the *i-t* test. The CV curves were recorded in N_2-saturated 0.25 M HCOOH + 0.5 M H_2SO_4 at a scan rate of 50 mV s^{-1}. It can be inferred that after the long-term *i-t* test, the Pt/C-SO_3^{2-} catalyst retained most of its catalytic activity, showing only a slight decrease in the current density at 0.55 V (0.48→0.39 A mg^{-1}) or the peak (0.89→0.83 A mg^{-1}).

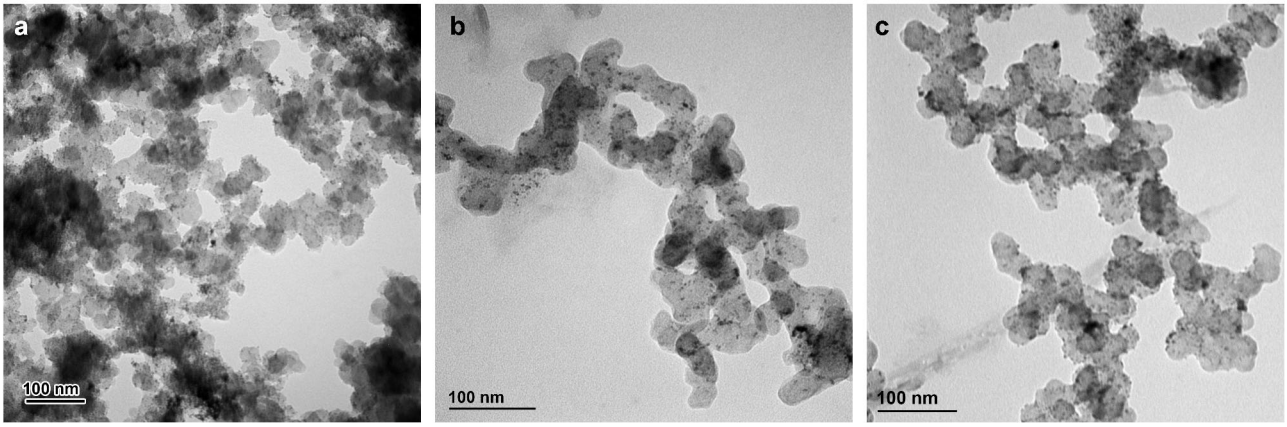

Fig. S10 TEM images of the Pt/C (a), the Pt/C-SO_3^{2-} as prepared, and the Pt/C-SO_3^{2-} after 1 h of the *i–t* test at 0.345 V vs. RHE.

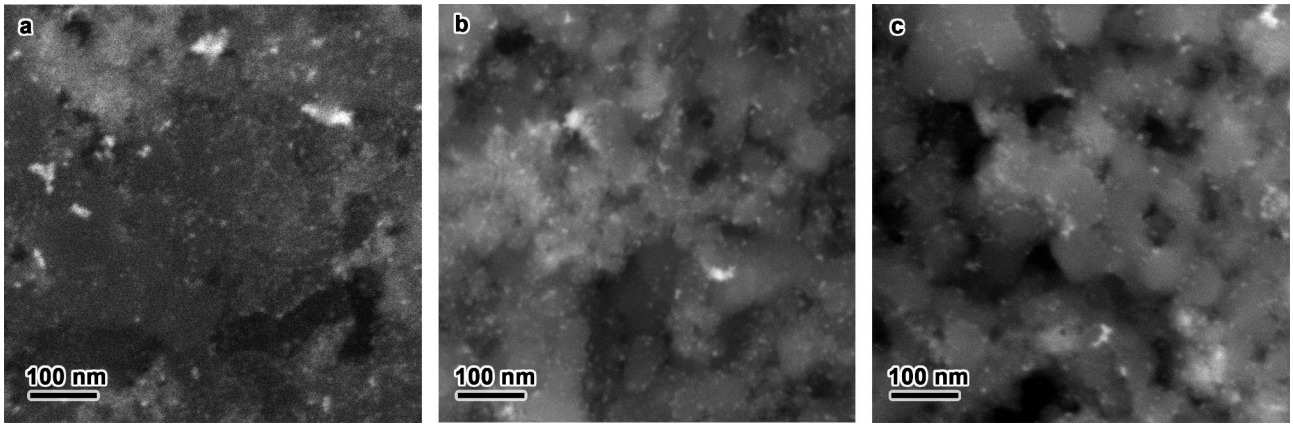

Fig. S11 SEM images of the Pt/C (a), the Pt/C-SO_3^{2-} as prepared, and the Pt/C-SO_3^{2-} after 1 h of the *i–t* test at 0.345 V vs. RHE. The images were taken by backscattered electron imaging. The white dots are images of the Pt nanoparticles.

Table S3. Comparison of the electrocatalytic activity of the Pt/C-SO_3^{2-} catalyst with those reported in the literature.*

Catalysts	Electrolyte	Scan rate ($mV\ s^{-1}$)	Mass activity at peak ($A\ mg^{-1}$)	Year	Ref.
Pt/C-SO_3^{2-}	0.5 M H_2SO_4 + 0.25 M HCOOH	50	0.89	-	This work
Organic ligand modification					
Pt/RGO-PEI hybrids	0.5 M H_2SO_4 + 0.5 M HCOOH	50	0.25**	2015	[1]
Butylphenyl-Pt NPs	0.1 M H_2SO_4 + 0.1 M HCOOH	50	1.03	2012	[2]
Other reports					
PtCuNi eb-NFs	0.5 M H_2SO_4 + 0.5 M HCOOH	50	0.34	2020	[3]
$PtCu_3$	0.5 M H_2SO_4 + 0.25 M HCOOH	10	0.45	2020	[4]
Pt/Sb	0.1 M $HClO_4$ + 0.1 M HCOOH	50	0.309	2020	[5]
Cu_5Pt nanoframes	0.5 M H_2SO_4 + 1.0 M HCOOH	50	0.194	2019	[6]
$PtNi_3$ CNCs	0.5 M H_2SO_4 + 0.5 M HCOOH	50	0.38	2019	[7]
Pt-Fe-Mn UCNC NCs	0.5 M H_2SO_4 + 0.25 M HCOOH	50	0.36	2019	[8]
PtCuCo NFs	0.5 M H_2SO_4 + 0.25 M HCOOH	50	0.56	2019	[9]
AgPt alloy nanowires	0.5 M H_2SO_4 + 1.0 M HCOOH	50	0.159	2018	[10]
Pt-Mn-Cu RP	0.5 M H_2SO_4 + 0.25 M HCOOH	50	0.33	2017	[11]
np-$Pt_{60}Au_{40}$ alloy	0.5 M H_2SO_4 + 0.5 M HCOOH	-	0.321	2011	[12]
Pt(0.5)/Bi/Pt NP	0.1 M H_2SO_4 + 0.5 M HCOOH	10	1.38	2020	[13]
PtBi/C	0.1 M H_2SO_4 + 0.25 M HCOOH	50	9.06	2020	[14]
$Pt_{45}Sn_{25}Bi_{30}$ nanoplates	0.5 M H_2SO_4 + 1.0 M HCOOH	50	4.39	2019	[15]

Pt-Au/C-3	0.5 M H_2SO_4 + 1.0 M HCOOH	-	14.5	2018	[16]
Au-Ag@Pt nanowires	0.5 M H_2SO_4 + 0.25 M HCOOH	50	6.8	2018	[17]
Pt_1/ATO	0.1 M $HClO_4$ + 0.5 M HCOOH	50	9.16	2018	[18]
$AuPt_{0.05ML}$	0.1 M H_2SO_4 + 0.5 M HCOOH	50	62.6	2013	[19]
$L1_0$-$Co_{41}Pt_{44}Au_{15}$	0.1 M $HClO_4$ + 2.0 M HCOOH	50	11.97	2019	[20]
$Pt_{0.10}$^Au-1.9/C	0.5 M H_2SO_4 + 2.0 M HCOOH	20	7.5	2012	[21]

*In many reports, the conditions and the data acquisition methods for the FAOR measurements are quite different, which makes it difficult to precisely evaluate the performance of the catalysts. The values listed here are for qualitative evaluation only.

**: Estimated value, as no specific value was presented in the report.

Discussion: The Pt/C-SO_3^{2-} catalyst report in this work showed high mass activity in the FAOR, compared with the Pt catalysts modified by organic ligands and many other recently reported Pt-based catalysts. There are some other catalysts that showed extremely high catalytic activity. They were delicately designed and grown from a complicated “bottom-up” synthesis, and many of them contain a large fraction of other noble metals such as Au and Ag. This work aims to enhance the catalytic activity of commercially available catalysts, Pt/C for example, by a simple ligand adsorption treatment (“top-down”). This strategy is advantageous over the conventional syntheses in that it is directly applicable in the current infrastructure, easy to operate and scale-up, and free of toxic or organic compounds (thus environmentally friendly).

References

[1] X. Gao, Y. Li, Q. Zhang, S. Li, Y. Chen and J.-M. Lee, *J. Mater. Chem. A*, 2015, **3**, 12000-12004.

[2] Z. Y. Zhou, J. Ren, X. Kang, Y. Song, S. G. Sun and S. Chen, *Phys. Chem. Chem. Phys.*, 2012, **14**, 1412-1417.

[3] D. Gao, S. Yang, L. Xi, M. Risch, L. Song, Y. Lv, C. Li, C. Li and G. Chen, *Chem. Mater.*, 2020, **32**, 1581-1594.

[4] J. Geng, Z. Zhu, X. Bai, F. Li and J. Chen, *ACS Appl. Energy Mater.*, 2020, **3**, 1010-1016.

[5] Y. Zhang, M. Qiao, Y. Huang, Y. Zou, Z. Liu, L. Tao, Y. Li, C. L. Dong and S. Wang, *Research*, 2020, **2020**, 5487237.

[6] Y. Wang, X. Jiang, G. Fu, Y. Li, Y. Tang, J. M. Lee and Y. Tang, *ACS Appl. Mater. Interfaces*, 2019, **11**, 34869-34877.

[7] D. Gao, S. Li, Y. Lv, H. Zhuo, S. Zhao, L. Song, S. Yang, Y. Qin, C. Li, Q. Wei and G. Chen, *J. Catal.*, 2019, **376**, 87-100.

[8] C. Qin, A. Fan, X. Zhang, X. Dai, H. Sun, D. Ren, Z. Dong, Y. Wang, C. Luan, J. Y. Ye and S. G. Sun, *Nanoscale*, 2019, **11**, 9061-9075.

[9] S. Yang, S. Li, L. Song, Y. Lv, Z. Duan, C. Li, R. F. Praeg, D. Gao and G. Chen, *Nano Res.*, 2019, **12**, 2881-2888.

[10] X. Jiang, G. Fu, X. Wu, Y. Liu, M. Zhang, D. Sun, L. Xu and Y. Tang, *Nano Res.*, 2017, **11**, 499-510.

[11] C. Luan, Q. X. Zhou, Y. Wang, Y. Xiao, X. Dai, X. L. Huang and X. Zhang, *Small*, 2017, **13**.

[12] J. Xu, C. Zhang, X. Wang, H. Ji, C. Zhao, Y. Wang and Z. Zhang, *Green Chem.*, 2011, **13**.

[13] H. Lee, Y. Sohn and C. K. Rhee, *Langmuir*, 2020, **36**, 5359-5368.

[14] C. Y. Wang, Z. Y. Yu, G. Li, Q. T. Song, G. Li, C. X. Luo, S. H. Yin, B. A. Lu, C. Xiao, B. B. Xu, Z. Y. Zhou, N. Tian and S. G. Sun, *ChemElectroChem*, 2020, **7**, 239-245.

[15] S. Luo, W. Chen, Y. Cheng, X. Song, Q. Wu, L. Li, X. Wu, T. Wu, M. Li, Q. Yang, K. Deng and Z. Quan, *Adv. Mater.*, 2019, **31**, e1903683.

[16] H. Fan, M. Cheng, L. Wang, Y. Song, Y. Cui and R. Wang, *Nano Energy*, 2018, **48**, 1-9.

[17] S. Zhang, L. Zhang, Z. Liu, M. Liu, Q. Fan, K. Liu and C. Gao, *J. Mater. Chem. A*, 2018, **6**, 22161-22169.

[18] J. Kim, C.-W. Roh, S. K. Sahoo, S. Yang, J. Bae, J. W. Han and H. Lee, *Adv. Energy. Mater.*, 2018, **8**, 1701476.

[19] S. Yang and H. Lee, *ACS Catal.*, 2013, **3**, 437-443.

[20] J. Li, S. Z. Jilani, H. Lin, X. Liu, K. Wei, Y. Jia, P. Zhang, M. Chi, Y. J. Tong, Z. Xi and S. Sun, *Angew. Chem. Int. Ed.*, 2019, **58**, 11527-11533.

[21] G.-R. Zhang, D. Zhao, Y.-Y. Feng, B. Zhang, D. S. Su, G. Liu and B.-Q. Xu, *ACS Nano*, 2012, **6**, 2226-2236.